Journal of
Electrical and Electronic Materials

View Online CrossMark
Regular Paper

Phase Transition of Li_3PO_4 Solid Electrolyte for Secondary Batteries in Vacuum: A Real-Time Synchrotron X-ray Scattering Study

Dong-Hyeon Shin[1], Seung-Han Lee[2], Tae-Sik Cho[1,2*]

[1] Department of Nano Materials Science and Engineering, Kyungpook National University, Sangju 37224, Korea
[2] Department of Hydrogen & Renewable Energy, Kyungpook National University, Daegu 41566, Korea

Corresponding author(s): cts@knu.ac.kr (T. S. Cho)

Cite as J. Electr. Electron. Mater., 39(5), 487–492 (2026), DOI: https://doi.org/10.4313/JEEM.2026.39.5.5
Received May 6, 2026; Revised June 17, 2026; Accepted June 28, 2026

ABSTRACT: The phase transition of Li_3PO_4 solid electrolyte for secondary batteries in vacuum has been studied by using real-time synchrotron X-ray scattering. According to the vacuum heating results, the crystal β-Li_3PO_4 phase was stable only from room temperature to 400°C. The crystal γ-Li_3PO_4 phase appeared at 410°C and the crystal β-Li_3PO_4 phase completely disappeared at 430°C. The transition from the β-Li_3PO_4 to the γ-Li_3PO_4 phases occurred primarily at 410°C, which is 40°C lower than the transition temperature of 450°C in air. The decrease in the phase transition temperature in vacuum, compared to that in air, is attributed to a relatively high concentration of oxygen vacancies. As the isothermal annealing time at 390°C was increased to 8 hours, the β-Li_3PO_4 phase was completely transitioned into the γ-Li_3PO_4 phase. Our study revealed the detailed transition behavior from the β-Li_3PO_4 to the γ-Li_3PO_4 phases during real-time annealing in vacuum.

KEYWORDS: Li_3PO_4 solid electrolyte, Phase transition during heating and isothermal annealing, Vacuum condition, Real-time synchrotron X-ray scattering

1 Introduction

Lithium (Li)-ion batteries, which are mainly used in electric vehicles, have several problems. While high energy density batteries are important for extending the driving distance of electric vehicles, Li-ion batteries are constrained by their theoretical maximum capacity [1,2]. Additionally, Li-ion batteries pose safety risks due to the separator's vulnerability to impact, excessive current, or extreme temperatures. This damage can lead to a short circuit, triggering a rapid release of stored energy and subsequent thermal runaway. Subsequent vaporization of the liquid electrolyte can trigger a fire or explosion [1,3].

One of the approaches to address these issues is the all-solid-state battery, which eliminates the liquid electrolyte and separator, replacing them with a solid electrolyte [1,3]. All-solid-state batteries greatly simplify packaging design, enabling higher energy density per unit volume compared to conventional batteries [3]. Solid electrolytes are categorized into organic and inorganic types, with inorganic electrolytes further subdivided into oxide-based and sulfide-based systems [4–7]. Oxide-based materials exhibit excellent atmospheric stability but suffer from high interfacial resistance [4,5,7]. Lithium phosphate (Li_3PO_4) is regarded as a promising material for solid oxide-based electrolytes owing to its simple composition, ease of preparation, low melting

points, and excellent glass-forming ability [8,9]. The Li_3PO_4 exists in three phases: β-Li_3PO_4, γ-Li_3PO_4, and α-Li_3PO_4 [10,11]. The space lattice of the three phases is orthorhombic [12,13]. The phase transition from β-Li_3PO_4 to γ-Li_3PO_4 is known to occur between 340°C and 580°C [8,10,11]. The phase transition from γ-Li_3PO_4 to α-Li_3PO_4 occurs at a high temperature of 1,170°C [10]. The Li_3PO_4 melted at 1,206°C [14].

Synchrotron X-ray scattering with very high flux and high resolution is one of the best ways to examine the detailed behaviors of nanomaterials during real-time annealing [15,16]. The phase transition from β-Li_3PO_4 to γ-Li_3PO_4 is significant, as the γ-Li_3PO_4 phase exhibits superior ionic conductivity compared to β-Li_3PO_4 phase [9]. However, the phase transition from β-Li_3PO_4 to γ-Li_3PO_4 during real-time annealing has not been well characterized. We have reported the transition behavior from β-Li_3PO_4 to γ-Li_3PO_4 phases during annealing in air using a real-time synchrotron X-ray scattering [17]. This paper further investigates the transition behavior from β-Li_3PO_4 to γ-Li_3PO_4 phases during annealing in vacuum and compares the results with those obtained in air.

2 Experimental Details

Li_3PO_4 powders (99.9%, Toshima manufacturing Co., Japan) were prepared via solid-state reaction. The Li_3PO_4 was synthesized by reacting Li_2O and P_2O_5 in a 3:1 molar ratio. The mixture was gradually heated up to 775°C, and the resulting melt was quenched into nitrogen to obtain granular pieces of Li_3PO_4.

The real-time synchrotron X-ray scattering experiments were performed at beamline 5D of the Pohang Light Source in Korea. The incident X-rays were vertically focused by a mirror and monochromatized to a wavelength of 1.240 Å for the measurements. The Li_3PO_4 solid electrolyte powders were annealed using a heating stage, which was set on a four-circle X-ray diffractometer. We precisely measured the integrated intensity of Bragg reflections by employing the Gaussian peak function. The heating annealing experiment was performed by measuring the X-ray diffraction profiles as a function of annealing temperature from room temperature (RT) to 600°C in vacuum. The isothermal annealing experiment was performed by measuring the X-ray diffraction profiles as a function of annealing time at 390°C in vacuum. In the meanwhile, the micrographs of Li_3PO_4 solid electrolyte powders before and after annealing were investigated by scanning electron microscope (SEM). To measure the particle sizes quantitatively, we used a particle size analyzer. We conducted additional SEM-EDS analysis after heat-treating the samples at 600°C for 30 min both in vacuum and in air. In vacuum, the sample showed P 23.11 and O 76.89 at% (n = 3), whereas in air, it showed P 22.91 and O 77.09 at% (n = 3).

3 Results and Discussion

Figure 1 shows the synchrotron X-ray diffraction profiles of the Li_3PO_4 solid electrolyte at several temperatures during heating in vacuum. At RT, the β-Li_3PO_4(110), β-Li_3PO_4(101), and β-Li_3PO_4(011) Bragg reflections were observed at q_z = 1.581 Å^{-1}, q_z = 1.656 Å^{-1} and q_z = 1.769 Å^{-1}, respectively [JCPDS No. 71-1528]. With increasing the annealing temperature to 400°C, only the β-Li_3PO_4 reflections were observed. At 410°C, in addition to β-Li_3PO_4 reflections, the γ-Li_3PO_4(012), γ-Li_3PO_4(110), and γ-Li_3PO_4(102) Bragg reflections appeared at q_z = 1.567, q_z = 1.626, and q_z = 1.74 Å^{-1}, respectively [JCPDS No. 84-0003]. At 430°C,

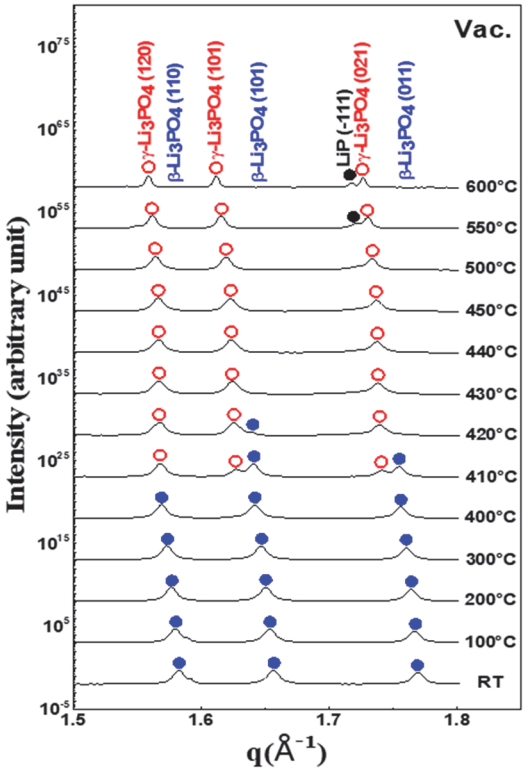

Fig. 1. Synchrotron X-ray diffraction profiles of the Li_3PO_4 solid electrolyte at several temperatures during real-time annealing in vacuum

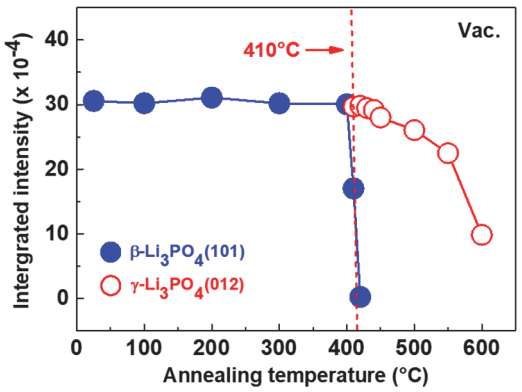

Fig. 2. X-ray integrated intensities of β-Li_3PO_4(101) and γ-Li_3PO_4(012) crystal phases in the Li_3PO_4 solid electrolyte as a function of annealing temperature in vacuum

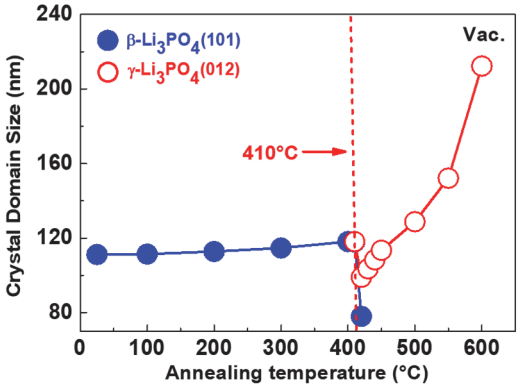

Fig. 3. Crystal domain sizes of the β-Li_3PO_4 and the γ-Li_3PO_4 phases in the Li_3PO_4 solid electrolyte as a function of annealing temperature in vacuum

only the γ-Li_3PO_4 reflections were observed and the β-Li_3PO_4 reflections wholly disappeared. The γ-Li_3PO_4 reflections were observed up to 600°C. In addition to γ-Li_3PO_4 reflections, LiP(-111) Bragg reflection observed at q_z = 1.718 $Å^{-1}$ at 550°C [JCPDS No. 83-1575]. After cooling to RT, only the γ-Li_3PO_4 reflections were observed (data-not shown). These indicate the transition from the β-Li_3PO_4 to the γ-Li_3PO_4 crystal phases near 410°C.

Figure 2 shows the X-ray integrated intensities of β-Li_3PO_4(101) and γ-Li_3PO_4(012) crystal phases as a function of annealing temperature in vacuum. The integrated intensity stands for the amount of crystal phase quantitatively [15,16]. As the annealing temperature increased to 400°C, the amount of β-Li_3PO_4 phase remained nearly constant. However, at 410°C, the amount of the β-Li_3PO_4 phase rapidly decreased, and the amount of the γ-Li_3PO_4 phase was similar to that of β-Li_3PO_4 phase. The β-Li_3PO_4 phase completely disappeared at 430°C. This clearly indicates that the phase transition from β-Li_3PO_4 to γ-Li_3PO_4 primarily occurred at 410°C. Also, the phase transition from β-Li_3PO_4 to γ-Li_3PO_4 occurred at 410°C in vacuum, which is 40°C lower than the transition temperature in air, 450°C. This reduction in transition temperature is attributed to a higher concentration of oxygen vacancies induced by the vacuum environment. The oxygen content in the sample treated at 600°C for 30 min in vacuum was 0.20 at% lower than that in air, which is attributed to the increased presence of oxygen vacancies.

The crystal domain sizes in a particle were estimated from the full-widths at half-maximum (FWHMs) of the β-Li_3PO_4(101) and the γ-Li_3PO_4(012) Bragg reflections using Scherrer equation [18]. Figure 3 shows the crystal domain sizes of the β-Li_3PO_4 and the γ-Li_3PO_4 phases in the Li_3PO_4 solid electrolyte as a function of annealing temperature in vacuum. At RT, the crystal domain size of the β-Li_3PO_4 phase was 111 nm. As the temperature increased to 410°C, the crystal domain size of the β-Li_3PO_4 phase remained around 118 nm. Also, the crystal domain sizes of β-Li_3PO_4 and γ-Li_3PO_4 phases were equal at 118 nm at 410°C. At 420°C, the crystal domain size of the β-Li_3PO_4 phase rapidly decreased to 78 nm. The crystal domain sizes of the γ-Li_3PO_4 phase gradually increased to 212 nm up to 600°C. These results indicate that the phase transition from β-Li_3PO_4 to γ-Li_3PO_4 primarily occurred at 410°C.

Although isothermal annealing was performed at 410°C, only the γ-Li_3PO_4 phase was present (data not shown). Therefore, we performed an isothermal annealing at 390°C, which is 20°C below 410°C. Figure 4 shows the synchrotron X-ray diffraction profiles of the Li_3PO_4 solid electrolyte at 390°C during isothermal annealing in vacuum. At RT, the β-Li_3PO_4(110), β-Li_3PO_4(101), and β-Li_3PO_4(011) Bragg reflections were observed [JCPDS No. 71-1528]. At 390°C, in addition to β-Li_3PO_4 reflections, the γ-Li_3PO_4(012), γ-Li_3PO_4(110), and γ-Li_3PO_4(102) Bragg reflections appeared [JCPDS No. 84-0003]. After 8 hours isothermal annealing, the β-Li_3PO_4 reflections disappeared. This indicates that the β-Li_3PO_4 phase had transitioned to the γ-Li_3PO_4 phase after 8 hours of isothermal annealing at 390°C in vacuum. The γ-Li_3PO_4 phase was observed for up to 9 hours.

Figure 5 shows the X-ray integrated intensities of the β-Li_3PO_4 and the γ-Li_3PO_4 phases in the Li_3PO_4 solid electrolyte as a function of isothermal annealing times at 390°C in vacuum. At 390°C, the γ-Li_3PO_4 phase coexisted with the β-Li_3PO_4 phase. The amount of

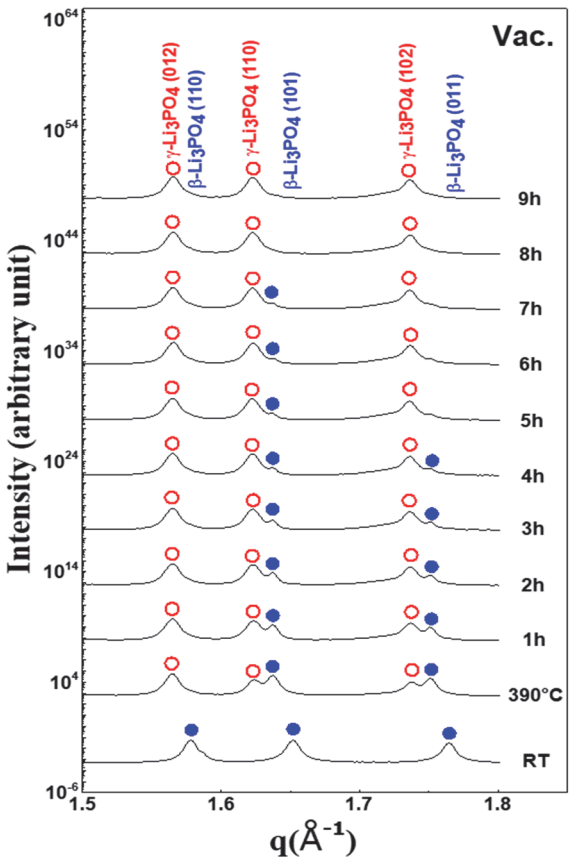

Fig. 4. Synchrotron X-ray diffraction profiles of the Li_3PO_4 solid electrolyte at 390°C during isothermal annealing in vacuum

the β-Li_3PO_4 phase decreased rapidly within the first 4 hours, followed by a slight decrease up to 7 hours, and completely disappeared after 8 hours. The amount of the γ-Li_3PO_4 crystal phase slightly increased up to 9 hours. These results indicate the phase transition from the β-Li_3PO_4 to the γ-Li_3PO_4 during isothermal annealing at 390°C in vacuum.

Figure 6 shows the crystal domain sizes of the β-Li_3PO_4 and the γ-Li_3PO_4 phases in the Li_3PO_4 solid electrolyte as a function of isothermal annealing times at 390°C in vacuum. At 390°C, the crystal domain size of the β-Li_3PO_4 phase was 109 nm. The crystal domain sizes of the β-Li_3PO_4 phase significantly decreased to 81 nm after 7 hours. The β-Li_3PO_4 phase disappeared after 8 hours. The crystal domain size of the γ-Li_3PO_4 phase, initially 93 nm after 1 hour, gradually increased to 102 nm by 9 hours. The change in crystal domain sizes was attributed to the phase transition from the β-Li_3PO_4 to the γ-Li_3PO_4 during isothermal annealing at 390°C in vacuum.

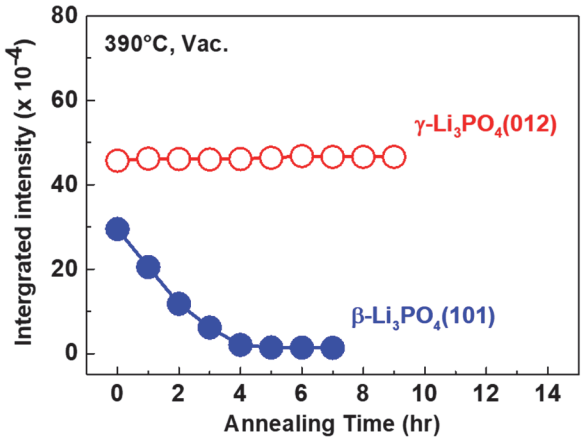

Fig. 5. X-ray integrated intensities of the β-Li_3PO_4 and the γ-Li_3PO_4 phases as a function of isothermal annealing times at 390°C in vacuum

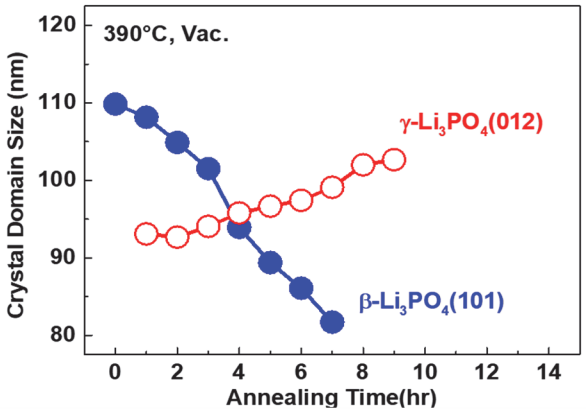

Fig. 6. Crystal domain sizes of the β-Li_3PO_4 and the γ-Li_3PO_4 phases in the Li_3PO_4 solid electrolyte as a function of isothermal annealing times at 390°C in vacuum

Figure 7 shows the SEM micrographs of the Li_3PO_4 solid electrolyte (a) before annealing at RT and (b) after annealing at 600°C in vacuum. As shown in Fig. 7(a), the Li_3PO_4 powders consist of small spherical particles. The mean particle size of the Li_3PO_4 powders was 250 nm. As illustrated in Fig. 7(b), the Li_3PO_4 powders transformed into a mixture of small spheres and large polygonal structures. After annealing at 600°C in vacuum, the mean particle size of the Li_3PO_4 powders significantly increased to 440 nm.

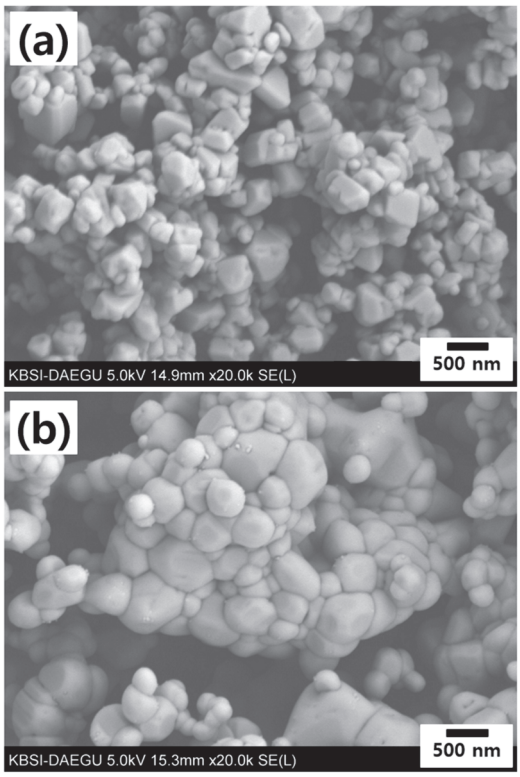

Fig. 7. SEM micrographs of the Li_3PO_4 solid electrolyte (a) before annealing at RT and (b) after annealing at 600°C in vacuum

4 Conclusion

We have studied the phase transition of Li_3PO_4 solid electrolyte for secondary batteries during heating and isothermal annealing in vacuum using real-time synchrotron X-ray scattering. According to the vacuum heating results, the crystal β-Li_3PO_4 phase was stable only from RT to 400°C. The crystal γ-Li_3PO_4 phase appeared at 410°C and the crystal β-Li_3PO_4 phase completely disappeared at 430°C. The phase transition from the β-Li_3PO_4 to the γ-Li_3PO_4 occurred primarily at 410°C, which is 40°C lower than the transition temperature of 450°C in air. The decrease in the phase transition temperature in vacuum, compared to that in air, is attributed to a relatively high concentration of oxygen vacancies. During the isothermal annealing at 390°C in vacuum, the amount of the β-Li_3PO_4 phase decreased rapidly within the first 4 hours, followed by a slight decrease up to 7 hours, and completely disappeared after 8 hours. Our study revealed the detailed transition behavior from the β-Li_3PO_4 to the γ-Li_3PO_4 phases during heating and isothermal annealing in vacuum.

ORCID

Tae-Sik Cho https://orcid.org/0000-0002-6619-152X

Acknowledgement

This research was supported by Kyungpook National University. This research was helped by Pohang Accelerator Laboratory in Korea. The authors also acknowledge Mr. K. J. Hwang for his contribution to SEM-EDS experiments in the Korean Basic Science Institute (Busan Center).

Conflict of Interest

The authors have no conflicts of interest to declare.

Author Contributions

Dong-Hyeon Shin: Conceptualization, Data curation, Visualization, Investigation, Formal analysis, Writing – original draft.
Seung-Han Lee: Visualization, Investigation.
Tae-Sik Cho: Conceptualization, Data curation, Visualization, Investigation, Formal analysis, Funding acquisition, Methodology, Project administration, Resources, Software, Supervision, Validation, Writing – review & editing.

Data Availability

Data available on request from the authors.

References

[1] S. S. Suh, C. W. Yi, and K. Kim, *J. Korean Electrochem. Soc.*, **15**, 1 (2012).
doi: https://doi.org/10.5229/JKES.2012.15.1.001
[2] F. Zheng, M. Kotobuki, S. Song, M. O. Lai, and L. Lu, *J. Power Sources,* **389**, 198 (2018).
doi: https://doi.org/10.1016/j.jpowsour.2018.04.022
[3] K. Takada, *J. Power Sources,* **394**, 74 (2018).
doi: https://doi.org/10.1016/j.jpowsour.2018.05.003

[4] B. W. Kang, H. T. Park, S. J. Woo, M. S. Kang, and A. Kim, *Ceramist,* **21**, 349 (2018).
doi: https://doi.org/10.31613/ceramist.2018.21.4.04
[5] M. Shoji, E. J. Cheng, T. Kimura, and K. Kanamura, *J. Phys. D Appl. Phys.,* **52**, 103001 (2019).
doi: https://doi.org/10.1088/1361-6463/aaf7e2
[6] N. Boaretto, I. Garbayo, S. Valiyaveettil-SobhanRaj, A. Quintela, C. Li, M. Casas-Cabanas, and F. Aguesse, *J. Power Sources,* **502**, 229919 (2021).
doi: https://doi.org/10.1016/j.jpowsour.2021.229919
[7] T. Schmaltz, F. Hartmann, T. Wicke, L. Weymann, C. Neef, and J. Janek, *Adv. Energy Mater.,* **13**, 2301886 (2023).
doi: https://doi.org/10.1002/aenm.202301886
[8] N. Ishigaki and J. Akimoto, *J. Asian Ceram. Soc.,* **9**, 452 (2021).
doi: https://doi.org/10.1080/21870764.2021.1891662
[9] N. I. P. Ayu, E. Kartini, L. D. Prayogi, M. Faisal, and Supardi, *Ionics,* **22**, 1051 (2016).
doi: https://doi.org/10.1007/s11581-016-1643-z
[10] L. Popović, B. Manoun, D. De Waal, M. K. Nieuwoudt, and J. D. Comins, *J. Raman Spectrosc.,* **34**, 77 (2003).
doi: https://doi.org/10.1002/jrs.954
[11] G. Torres-Treviño and A. R. West, *J. Solid State Chem.,* **61**, 56 (1986).
doi: https://doi.org/10.1016/0022-4596(86)90006-X
[12] Y. A. Du and N. A. W. Holzwarth, *J. Electrochem. Soc.,* **154**, A999 (2007).
doi: https://doi.org/10.1149/1.2772200
[13] R. K. Osterheld, *J. Inorg. Nucl. Chem.,* **30**, 3173 (1968).
doi: https://doi.org/10.1016/0022-1902(68)80109-5
[14] L. Zhang, New Li+ Ion Conducting Solid Electrolytes Based on the LISICON Structure, *Ph.D. thesis*, Queen Mary University of London, London, UK (2020).
https://qmro.qmul.ac.uk/xmlui/handle/123456789/71995
[15] J. H. Jeong and T. S. Cho, *J. Nanoscience Nanotechnol.,* **17**, 7799 (2017).
doi: https://doi.org/10.1166/jnn.2017.14846
[16] T. S. Cho, J. H. Je, and D. Y. Noh, *Appl. Phys. Lett.,* **76**, 303 (2000).
doi: https://doi.org/10.1063/1.125727
[17] D. H. Shin, S. H. Lee, and T. S. Cho, *Sci. Adv. Mater.,* **16**, 1238 (2024).
doi: https://doi.org/10.1166/sam.2024.4737
[18] B. E. Warren, *X-Ray Diffraction*, 1st edn. (Dover Publications, New York, 1969).